Ecological Informatics 95 (2026) 103728

Contents lists available at ScienceDirect

Ecological Informatics

journal homepage: www.elsevier.com/locate/ecolinf

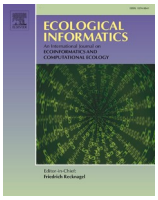

Automated morphometric analysis and biomass estimation of marine nematodes using a conical frustum segmentation approach

Harshpreet Kaur [a,b], Arjunveer Singh [a,b], Daniel Jones [c], Pedro Martinez Arbizu [d], Ravail Singh [a,b,c,*]

[a] CSIR-Indian Institute of Integrative Medicine (IIIM), Jammu 180001, Jammu & Kashmir, India
[b] Academy of Scientific and Innovative Research (AcSIR), Ghaziabad 201002, India
[c] National Oceanography Center, Southampton SO14 3ZH, United Kingdom
[d] Senckeneberg Institute of Biodiversity, Wilhelmshaven 26382, Germany

ARTICLE INFO

Keywords:
Nematodes
Biomass
New method
RAH NemaCalc
Python-based
Frustum

ABSTRACT

Marine nematodes, the most abundant meiofauna in benthic ecosystems, drive critical nutrient cycling and carbon sequestration, yet accurate biomass estimation remains challenging due to morphological variability and reliance on simplistic geometric models like Andrássy's formula, which introduced systematic biases across taxa. This study developed RAH NemaCalc, an open-source Python-based tool with Tkinter GUI and OpenCV integration that semi-automates morphometric analysis by segmenting nematodes into 5–20 conical frustums based on length-diameter ratios, calculating lateral surface area with morphology-specific correction factors (k_{total} and frustum geometry factor f), and converting to biomass using an empirically determined density of 1.08 g/cm^3 derived from sucrose gradient centrifugation of 50 genera. The tool processed high-resolution images of 187 specimens from diverse habitats- 50 from Lakshadweep Islands, 87 from Clarion Clipperton Zone abyssal sediments, and 50 from the Nemys database yielding processing times of 1.8–2.1 s/image with manual contour verification. Key results showed the frustum method produced significantly different biomass estimates from Andrássy (Wilcoxon $p < 0.0001$ across datasets), with median volume reductions of 20–28% in coastal/abyssal samples but up to 260% higher biomass in large tapered genera like *Linhomoeus* and *Halichoanolaimus*; Bland-Altman analysis confirmed morphology- and size-dependent bias, while 10–20 segments optimized accuracy for tapered forms. RAH NemaCalc thus established a precise, high-throughput standard for nematode biomass quantification, enabling reliable monitoring of anthropogenic impacts like deep-sea mining on ecosystem functions and informing conservation baselines.

1. Introduction

Marine nematodes are microscopic roundworms inhabiting benthic ecosystems, represent one of the most abundant and functionally important meiofaunal groups, accounting for up to 90% of sediment dwelling organisms (Singh et al., 2014, 2016; Zeppilli et al., 2018). Their unparalleled diversity and metabolic activity make them critical drivers of nutrient cycling, organic matter decomposition, and energy transfer in marine food webs (Giere, 2009; Schratzberger and Ingels, 2018). By mediating carbon sequestration and regenerating nitrogen and phosphorus, nematodes sustain primary productivity and underpin ecosystem stability with direct implications for fisheries and global biogeochemical cycles (Danovaro et al., 2020; Heip et al., 1985).

Despite their ecological significance, marine nematodes face escalating threats from anthropogenic disturbances. In coastal zones, pollution and ocean acidification disrupt community structures (Zeppilli et al., 2018) while deep-sea mining in regions like the Clarion Clipperton Zone (CCZ) and the Indian Ocean generates sediment plumes and habitat destruction with recovery timelines spanning decades (Jones et al., 2017; Miljutin et al., 2011; Singh et al., 2019). Climate change further exacerbates these pressures by altering temperature and oxygen regimes, potentially destabilizing nematode-mediated ecosystem functions (Snelgrove et al., 2018). The biomass of nematodes is particularly important in this context because it serves as a direct measure of their abundance and activity, which underpins their critical roles in nutrient cycling, energy transfer, and overall ecosystem stability. Changes in

* Corresponding author.
E-mail address: Ravail.Singh@noc.ac.uk (R. Singh).

https://doi.org/10.1016/j.ecoinf.2026.103728
Received 6 August 2025; Received in revised form 17 March 2026; Accepted 17 March 2026
Available online 19 March 2026
1574-9541/© 2026 The Authors. Published by Elsevier B.V. This is an open access article under the CC BY license (http://creativecommons.org/licenses/by/4.0/).

nematode biomass can signal environmental stress such as pollution or deep-sea mining impacts before larger organisms are affected. Accurate biomass data are therefore essential not only for understanding nematode population dynamics but also for monitoring ecosystem health and informing conservation strategies, as declines in nematode biomass can indicate the loss of critical ecological functions. However, existing biomass estimation methods remain prone to error and inadequacy, limiting effective ecological assessment. Traditional approaches, such as Andrássy's formula (1956), rely on simplistic geometric models (e.g., uniform cylinders or cuboids) and manual measurements of length and diameter. These methods are labour-intensive, subjective, and often destructive, preventing further taxonomic or genetic analysis (Feller and Warwick, 1988). More fundamentally, they fail to accommodate morphological diversity, systematically underestimating biomass in tapered taxa (e.g., *Linhomoeus*) and overestimating it in slender cylindrical forms (Fonseca and Soltwedel, 2007; Mazurkiewicz et al., 2016; Vanaverbeke et al., 2003).

In response, semi-automated tools such as ImageJ (Schindelin et al., 2012) and taxon-specific databases like NINJA (Sieriebriennikov et al., 2014) have improved measurement efficiency but retain oversimplified geometric assumptions. While NINJA automates biomass calculation using preexisting taxon-specific mass data, it lacks adaptability to marine nematode morphology and depends on generalized values that may not reflect environmental or intraspecific variation. Other refinements, including taxon-specific corrections (Mazurkiewicz et al., 2016) and diameter-only formulas (Zhao et al., 2019), either require extensive calibration or trade accuracy for simplicity. Although efforts such as the semi-automated image analysis of Baguley et al. (2004) represent progress, they continue to rely on cylindrical approximations that do not resolve core geometric limitations. Consequently, a significant methodological gap persists, undermining large scale ecological monitoring particularly in marine systems where nematodes serve as vital bioindicators of environmental change (Ridall and Ingels, 2021).

To address these critical methodological gaps and safeguard nematodes' ecological functions, we developed RAH NemaCalc, a Python-based, open source tool that revolutionizes biomass estimation. This computational solution advances upon traditional geometric approximations (e.g., Andrassy's formula) by automatically decomposing nematode morphologies into conical frustums, enabling precise calculation of lateral surface area and biomass while accounting for interspecific morphological variation. Initial validation using 187 specimens from diverse benthic environments including abyssal sediments of the Clarion Clipperton Zone and coastal systems of Androth and Elikalpeni Island demonstrates significant improvements in both accuracy and processing efficiency compared to conventional methods. The non-destructive, high throughput nature of this approach facilitates reliable biomass quantification at ecologically relevant scales, providing critical data for monitoring anthropogenic impacts on marine ecosystems. This methodological innovation establishes a new standard for studying nematode-mediated ecosystem processes while supporting evidence-based conservation management.

2. Materials and methods

2.1. Nematode genera dataset

Three nematode datasets were used to test the RAH NemaCalc software. The first dataset comprised 50 specimens from 34 genera gathered from diverse habitats including rocky, rock/sediment, and sandy substrates at Elikalpeni (West and East) and Androth in the Lakshadweep Islands, Indian Ocean. The second dataset consisted of 87 specimens from 41 genera, collected from the Clarion Clipperton Zone (CCZ) in the Pacific Ocean (11–14°N, 116–120°W) at depths of 4100–4400 m. The third dataset was obtained from the open source Nemys image database, from which 50 high-quality images representing 50 genera were selected for testing purposes. High resolution digital images of all specimens were compiled into a database for software analysis (Supplementary file 1).

Manual measurements of length, diameter, and volume were conducted for each specimen from all datasets using a Leica LAS EZ microscope. Volume was calculated using Andrassy's formula: $V = (L \times D^2) / 1.7$, with biomass derived as $(L \times D^2)/(1.6 * 10^6)$. The images of all the nematodes of the dataset were taken and an image database of the nematodes was created.

We then developed a new formula for biomass calculation of nematodes. The formula uses lateral surface area instead of volume. The nematodes were treated as various segments of frustums of cones and for each segment the lateral surface area was calculated and the lateral surface area of all the segments was summed up to generate a total lateral surface area for the whole nematode body (Fig.1). The LSA of one segment was calculated using the formula:

$$AL = \pi^{*} (r_1 + r_2)^{*} l$$

where, AL is the lateral surface area.

r_1 and r_2 are the radii of the larger and smaller bases.

l is the slant height with formula $\sqrt{(h^2 + (r1 - r2)^2)}$ (h is the vertical height of the frustum of cone.)

Due to different morphological aspects attributed to different genera of nematodes leading to misrepresentation of biomass as depicted in Fig. 2, to facilitate and overcome this misinterpretation or exaggeration of biomass values we have incorporated a correction factor k_{total} into the formula as depicted in Fig. 1

$$k_{total} = ½^{*}⅓ \left((ra^2 + ra.rb + rb^2)/(ra + rb)\right)$$
$$= (1/6) \left((ra^2 + ra.rb + rb^2)/(ra + rb)\right); ra$$
$$= \text{Radius of posterior end of nematode, rb}$$
$$= \text{Radius of anterior end of nematode}$$

k_{total} combines two adjustments for the entire nematode, using terminal radii r_a and r_b:

Taper Adjustment Factor (½) and Thickness Adjustment Factor.

For the taper, l (slant height) = 2 h (Total vertical height).

h/l = ½ which adjusts for the tapering from posterior end to the anterior end.

For the thickness: Volume (V) = k. Lateral Surface Area (LSA)

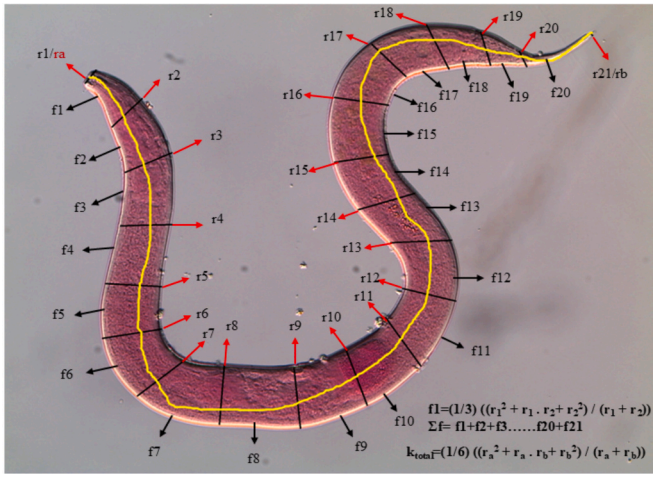

Fig. 1. Image illustrating nematode segmentation in NemaCalc software for morphometric analysis. The nematode is segmented into conical frustums with each segment having radii (r1 to r21) and conversion factor (f1 to f20) summed as Σf. Each conversion factor (f1 to f20) makes use of their respective segments' radius (r1 to r21). The total of all the conversion factors (f1 + f2… + f19 + f20) is represented by Σf. The correction factor k total uses only the anterior and posterior radii (ra and rb), treating nematodes as linear structure.

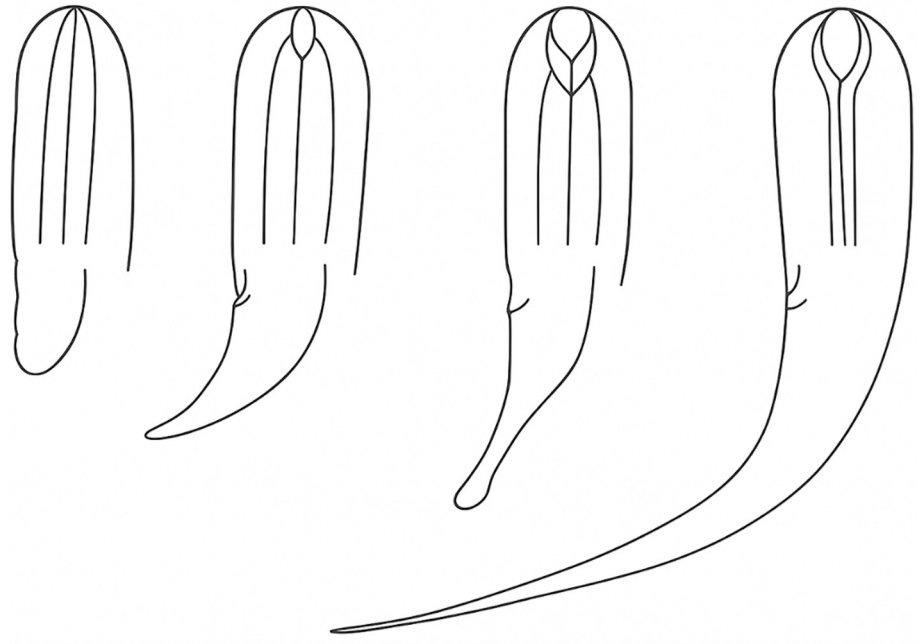

Fig. 2. The diagram illustrates the diverse shapes of buccal cavities and tails in nematodes, which are critical factors contributing to the varied tapering forms observed in their body structure

$$\frac{1}{3}\,\pi\,h\left(r_a{}^2 + r_a.r_b + r_b{}^2\right) = k.\pi(r_a + r_b).l$$

$k = h/3\ l\ (r_a^2 + r_a.r_b + r_b^2)/(r_a + r_b)$,

Considering tapering in nematodes $h = l$ and hence,

$k = {}^1\!/_3\ ((r_a^2 + r_a.r_b + r_b^2)\ /\ (r_a + r_b))$ (Thickness Adjustment Factor).

Combining both adjustments gives $k_{total} = (1/6)\ ((r_a^2 + r_a.r_b + r_b^2)\ /\ (r_a + r_b))$.

The formula for biomass of nematodes was then computed as:

$$W = \pi\, k_{total}\, \rho\, \Sigma\, AL.f\ (\text{The Arjun} - \text{Preet} - \text{Ravail Formula})$$

where f = Frustum Geometry Factor = $(1/3)\ (((r_1^2 + r_1.\ r_2 + r_2^2))\ /\ (r_1 + r_2))$; r_1 and r_2 = radii of the larger and smaller bases.

$$V = f{\cdot}LSA \geq f = V/LSA \geq \frac{1}{3}\,\pi h\left(r_1{}^2 + r_1.r_2 + r_2{}^2\right)/\pi(r_1 + r_2).l.$$

For minimal taper in each segment, $l \approx h$, so $r_1 \approx r_2$.

So, $f = (1/3)\ ((r_1^2 + r_1.\ r_2 + r_2^2)\ /\ (r_1 + r_2))$.where $\rho = 1.08 \times 10^{-6}$ μg/μm^3 (density = 1.08 g/cm^3), the value for density was also experimentally determined by calculating the specific gravity of the nematodes. Specific gravity was determined using density gradient centrifugation with sucrose solutions (20–80% and 30–120% *w/v*). For each gradient, 0.5 ml of sucrose solution was made with the optimum amount of sucrose for each percentage (e.g., 0.1 g sucrose in 0.5 ml Milli Q for 20% solution). The density was measured with a Brix Refractometer and then the nematodes were added on the top layer of the solution under a stereomicroscope. Nematodes were centrifuged at 2000 ×*g* for 10 min, yielding specific gravity of 1.05–1.15; then its density was calculated via:

$$\text{Specific Gravity} = \text{Density of Nematode}/\text{Density of Water}$$

A mean value was calculated for the software which gave the density of 1.08 g/cm^3.

Apart from biomass, our software also uses a new method for calculation of volume of nematodes using segmentation approach and considering nematodes as frustums of cones. The formula used for volume was:

$$V = \frac{1}{3}\pi h\left(r_1{}^2 + r_1.r_2 + r_2{}^2\right)$$

These measurements served as a reference for developing RAH NemaCalc, which processes the compiled image database to semi-automate morphometric analysis, segmenting nematodes into conical frustums for precise biomass estimation.

2.2. Software development

RAH NemaCalc was developed in Python 3.x as a specialized tool for nematode morphometric analysis and biomass estimation. The software architecture integrates core libraries: Tkinter for the graphical user interface, OpenCV for image processing, and PIL for image display and conversion (Supplementary file 2).

The workflow consists of four key steps:

1. **Image Loading & Scale Calibration:** Users load an image and draw a reference line of known length. The software calculates pixels per micrometre using the Pythagorean Theorem, applying this scale to all subsequent measurements.
2. **Measurement & Segmentation:** The interface supports linear and freehand measurement tools. For biomass estimation, users measure total nematode length, specify the number of frustum segments (5, 10, or 20), and input diameters at segment points along the body.
3. **Data Management:** Measurements are stored as named variables, with full undo/redo functionality and session management. Critical variables (length and diameter) are saved for automated calculation of volume, lateral surface area (LSA), and biomass via both Andrássy and frustum-based methods.
4. **Export & Output:** Results can be exported in multiple formats: CSV for tabular data, Excel for structured worksheets, PDF for comprehensive reports, and annotated images with measurement overlays. The interface features an interactive canvas with zoom/pan controls, keyboard shortcuts, and real time result display. Optimized algorithms ensure efficient processing (~2 s per specimen), while comprehensive error handling and validation maintain data integrity. The modular design allows for future expansion of measurement types and export formats.

2.3. Segmentation approach

Nematodes were segmented into 5, 10, or 20 frustums based on morphology, guided by length-diameter ratios: 5 segments for slender genera (ratio > 30, e.g., *Desmocolex*, *Amphimonhystrella*), 10 segments for moderately tapered genera (ratio 15–30, e.g., *Marylynnia*, *Viscosia*), and 20 segments for robust, highly tapered genera (ratio < 15, e.g., *Terschellingia*, *Linhomoeus*). Images were processed at ~5 s (1.8 s/image for 10 segments, 2.1 s for 20 segments), with contours manually verified to ensure accuracy.

This study employed a morphology driven biomass comparison to evaluate two biomass estimation methods, Andrassy and Frustum across nematode morphologies. The experimental design was a two-factor, fully crossed setup with 187 nematode specimens (50 from Androth/Elikalpeni, 87 from the CCZ, and 50 from Nemys), each measured using both methods. Factor 1 was the biomass estimation method (Andrassy vs. Frustum), and Factor 2 was nematode morphology, classified as either robust (length/diameter ratio, L/D < 15) or slender (L/D > 30). The primary response variable was biomass (µg). A regression analysis was conducted with the model: Biomass vs. L/D (Morphology). Post-hoc diagnostics included Bland-Altman analysis to assess agreement between methods (reporting bias and limits of agreement) and residual analysis for heteroscedasticity and outlier detection. This approach ensured robust statistical evaluation of method and morphology effects on biomass estimation, in line with best practices for methodological transparency and reproducibility.

2.4. Statistical analysis

The measured length, diameter, and frustum segments for 187 specimens were calculated. Biomass variability was assessed using regression analysis, and non-parametric statistical methods were used. Differences between Andrassy- and frustum-derived volume estimates were assessed using the Wilcoxon signed-rank test, applied separately for each dataset. Descriptive statistics, including mean values, median percentage differences, and coefficients of variation (CV), were calculated to characterize central tendency and dispersion. All analyses were performed on paired measurements derived from the same specimens. The effect of frustum segment number (5 vs. 20) was tested on an *Acantholaimus* specimen.

User Guide:

Getting Started with RAH NemaCalc.

A step-by-step manual for accurate, automated biomass estimation is presented in Fig.3. For complete reference to the user manual, refer to Supplementary file 3.

3. Results

3.1. Specific gravity insights

Specific gravity measurements using density gradient centrifugation (20–80% sucrose, 2000 ×g, 10 min) showed that 90% of the 50 specimens settled between the 40–60% sucrose layers in the first gradient, and 94% between the 30–60% layers in the second gradient. Using the relation Density = Specific Gravity × Density of Water (0.997 g/cm^3 at 25 °C), nematode densities ranged from 1.05 to 1.15 g/cm^3 across all 50 genera. Slender cylindrical genera such as *Microlaimus*, *Wieseria*, and *Mesacanthion* showed lower densities (1.05–1.07 g/cm^3), while moderately tapered forms (*Daptonema*, *Amphimonhystrella*, *Marylynnia*) ranged between 1.07 and 1.10 g/cm^3. Robust, strongly tapered, or cuticularized genera such as *Linhomoeus*, *Terschellingia*, *Halichoanolaimus*, and *Parasphaerolaimus* exhibited the highest densities (1.11–1.15 g/cm^3), showing a morphology dependent density pattern. Across all specimens, the biomass variation due to density differences was <±3.5%, indicating that density contributes minimally to estimation error compared to geometric factors (length, diameter, and tapering). Therefore, the mean experimentally derived density of 1.08 g/cm^3 was selected and applied uniformly in the software for all biomass calculations. (Table 1).

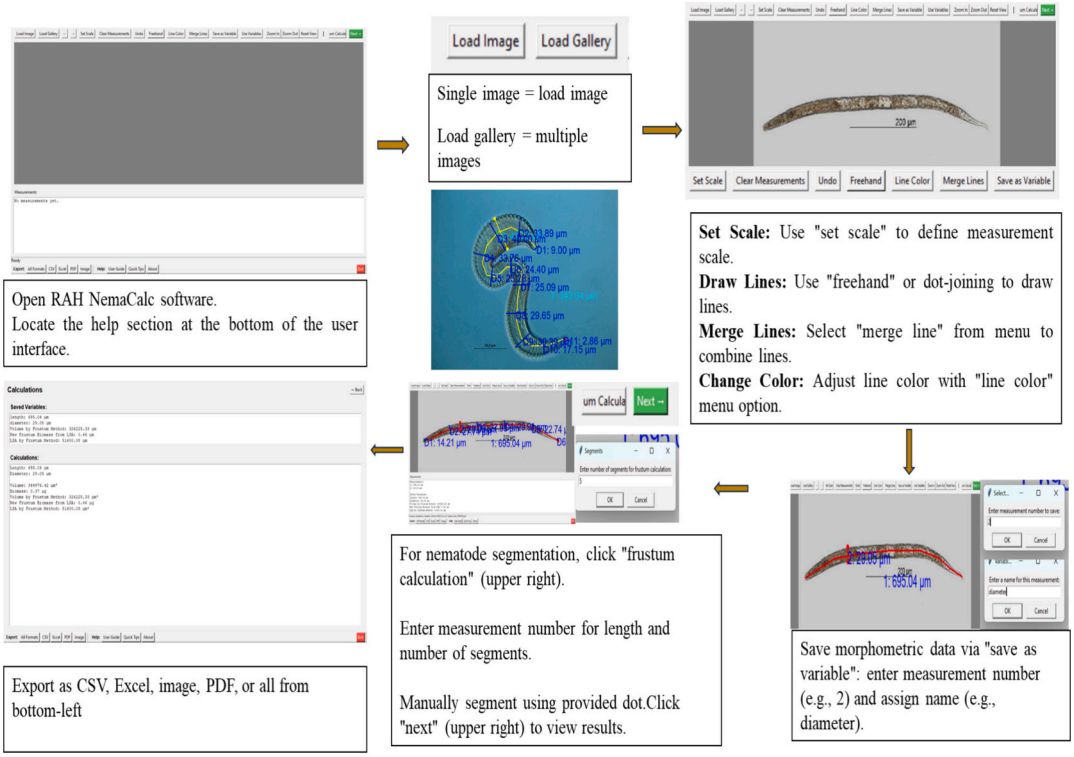

Fig. 3. Diagram illustrating the step-by-step morphometric analysis process in RAH NemaCalc software, depicting image loading, scale setting, nematode segmentation via frustum calculation, line drawing, merging, and coloring, data saving, result display, and export options, with reference to the help section for guidance.

Table 1
Equilibrium sucrose concentration, specific gravity, and density of different marine nematode genera and species.

No.	Genus Name	Equilibrium Sucrose (%)	Specific Gravity	Density (g/cm^3)
1	*Linhomoeus*	57	1.11	1.110
2	*Terschellingia*	60	1.12	1.120
3	*Halichoanolaimus*	58	1.11	1.110
4	*Sphaerolaimus*	59	1.12	1.120
5	*Anticoma*	56	1.11	1.110
6	*Camacolaimus*	55	1.10	1.100
7	*Greeffiella*	61	1.13	1.130
8	*Cervonema*	60	1.12	1.120
9	*Tripylidae*	59	1.12	1.120
10	*Parasphaerolaimus*	63	1.14	1.140
11	*Desmodora*	52	1.09	1.090
12	*Diplopeltula*	52	1.09	1.090
13	*Euchromadora*	53	1.09	1.090
14	*Cyatholaimus*	53	1.09	1.090
15	*Marylynnia*	52	1.09	1.090
16	*Viscosia*	51	1.08	1.080
17	*Daptonema*	50	1.08	1.080
18	*Disconema*	50	1.08	1.080
19	*Tarvaia*	49	1.08	1.080
20	*Oxystomina*	49	1.08	1.080
21	*Acantholaimus*	51	1.08	1.080
22	*Amphimonhystrella*	48	1.07	1.070
23	*Paramphimonhystrella*	49	1.08	1.080
24	*Oncholaimus*	47	1.07	1.070
25	*Sabatieria*	46	1.07	1.070
26	*Leptolaimus*	45	1.06	1.060
27	*Microlaimus*	44	1.06	1.060
28	*Mesacanthion*	44	1.06	1.060
29	*Thalassomonhystera*	44	1.06	1.060
30	*Wieseria*	45	1.06	1.060
31	*Tricoma*	43	1.05	1.050
32	*Metadesmolaimus*	43	1.05	1.050
33	*Metachromadora*	43	1.05	1.050
34	*Ceramonema*	43	1.05	1.050
35	*Chromadorita*	42	1.05	1.050
36	*Monhysteridae*	42	1.05	1.050
37	*Tripyloides*	47	1.07	1.070
38	*Richtersia*	50	1.08	1.080
39	*Halalaimus sp_1*	52	1.09	1.090
40	*Halalimus sp_2*	60	1.12	1.120
41	*Camacolaimus*	54	1.10	1.100
42	*Anticoma*	56	1.11	1.110
43	*Sphaerotheristus*	57	1.11	1.110
44	*Halichoanolaimus robustus*	58	1.12	1.120
45	*Camacolaimus_sp2*	55	1.10	1.100
46	*Tripylidae*	61	1.13	1.130
47	*Parasphaerolaimus* sp.	63	1.14	1.140
48	*Desmodora sp_2.*	64	1.15	1.150
49	*Onchium longispiculum*	57	1.11	1.110
50	*Desmocolex sp4*	45	1.07	1.070

3.2. Comparison of andrassy and frustum volume and biomass

RAH NemaCalc processed 187 nematode specimens collected from three ecologically distinct marine habitats: 50 specimens (34 genera) from rocky–sandy substrates of Androth/Elikalpeni, Indian Ocean; 87 specimens (41 genera) from polymetallic nodule-rich sediments of the Clarion–Clipperton Zone (CCZ), Pacific Ocean; and 50 morphologically diverse specimens extracted from global datasets (NEMYS Open Source), representing additional habitats and body plans not captured in field sampling. High-resolution calibrated images (1920 × 1080 px, ~2.1 MB each) were processed using the automated 10-frustum segmentation pipeline, with a mean computation time of 1.8 s/image for simultaneous extraction of length, diameter profiles, and frustum-based biomass.

Across all three datasets, the frustum-based method consistently produced lower mean volume estimates than the Andrassy method (Table 2). In the Androth/Elikalpeni dataset, mean Andrassy volume was 2.50×10^6 μm^3, whereas mean frustum volume was 1.24×10^6 μm^3, corresponding to a median volume reduction of 28.0%. Similarly, the CCZ dataset showed a median reduction of 26.5%, and the open-source dataset showed a median reduction of 20.3% when using the frustum method. Wilcoxon signed-rank tests indicated that these differences were highly significant in all datasets (Androth/Elikalpeni: Z = 7.00, $p < 0.0001$; CCZ: Z = 49.00, $p < 0.0001$; Open source: Z = 0.00, $p < 0.0001$), demonstrating a consistent systematic difference between the two volume estimation methods.

Table 2
Comparison of nematode volume and biomass estimates using Andrassy and Frustum methods across two study regions and an open source data: Androth/Elikalpeni ($n = 50$), the Clarion Clipperton Zone (CCZ, $n = 87$) and the Nemys data ($n = 50$).

Metric	Androth / Elikalpeni (n = 50)	CCZ (n = 87)	Open Source (n = 50)
Mean Andrassy Volume (μm^3)	2,501,298	1,738,010	115,757,416
Mean Frustum Volume (μm^3)	1,239,223	1,277,715	92,213,445
Median Volume Difference (%)	−28.0%	−26.5%	−20.3%
Wilcoxon Signed-Rank Z	7.00	49.00	0.00
Wilcoxon *p*-value	< 0.0001	< 0.0001	< 0.0001
Largest Genus Reduction	*Terschellingia*: +22,155.65	*Halichoanolaimus* sp.: +84,809.64	*Wieseria* sp.: −23,621.93
Coefficient of Variation – Andrassy	286.45%	156.68%	348.23%
Coefficient of Variation – Frustum	152.05%	145.73%	358.23%

Volume estimates exhibited substantial variability across specimens, reflected in large coefficients of variation for both methods. CVs for Andrassy-derived volumes ranged from 156.7% to 348.2%, while frustum-derived volumes ranged from 145.7% to 358.2%, indicating highly right-skewed distributions dominated by a small number of large-bodied specimens. The largest absolute differences between methods were associated with specific genera. In the Androth/Elikalpeni dataset, *Terschellingia* exhibited the greatest reduction in estimated volume. In the CCZ dataset, the largest difference was observed for *Halichoanolaimus* spp., while in the open source dataset, the largest difference occurred in *Wieseria* spp. (Table 2).

Wilcoxon tests confirmed systematic directional bias across all datasets ($p < 0.0001$), suggesting that the Andrassy formula consistently overestimates volume in tapered and segmented taxa. Largest genus-specific reductions were observed in CCZ (84,809 μm^3) and Androth (22,155 μm^3), highlighting that the degree of overestimation increases with body volume.

Biomass estimates obtained using the traditional Andrassy method and the novel APR (frustum-based) formula are summarized in Table 3 for each study region. In the Androth/Elikalpeni dataset ($n = 50$), the Andrassy method yielded a mean biomass of 1.70 ± 2.38 μg (median: 1.00 μg), whereas the APR formula produced a higher mean of 2.19 ± 4.17 μg (median: 0.72 μg). For the Clarion Clipperton Zone (CCZ) (n = 87), Andrassy-derived biomass averaged 1.85 ± 2.90 μg (median: 0.63 μg), compared to 2.25 ± 4.20 μg (median: 0.59 μg) with the APR method. The most pronounced differences were observed in the Open Source (Nemys) dataset (n = 50), where the Andrassy method gave a mean of 120.56 ± 424.24 μg (median: 6.01 μg), while the APR formula yielded a substantially higher mean of 371.92 ± 1494.83 μg (median: 7.54 μg). Across all regions, biomass distributions were highly right-skewed, as indicated by large standard deviations and maxima far exceeding median values, underscoring the influence of a few large-bodied taxa on community biomass estimates.

A closer examination reveals important and consistent biases that

Table 3
Summary statistics for nematode biomass (µg) estimated using Andrássy and the APR (Frustum-based) formula across three regions. Metrics include sample size (N), mean, standard deviation, median, and minimum-maximum ranges.

Region	Method	N	Mean (µg)	Standard Deviation (µg)	Median (µg)	Minimum (µg)	Maximum(µg)
	Andrassy	50	1.70	2.38	1.00	0.07	9.91
	The APR Formula	50	2.19	4.17	0.72	0.05	15.53
Androth/Elikalpeni							
	Andrassy	87	1.85	2.90	0.63	0.07	18.08
Clarion-Clipperton Zone (CCZ)	The APR Formula	87	2.25	4.20	0.59	0.04	22.25
	Andrassy	50	120.56	424.24	6.01	0.08	2445.87
Open Source (Nemys)	The APR Formula	50	371.92	1494.83	7.54	0.03	8310.78

vary with nematode morphology and size. To assess this statistically, correlation analysis was first used to understand scaling similarity between methods while agreement between methods was formally evaluated using Bland-Altman analysis. The regression line included in these plots was intended only to visualise scaling trends. The results show that strong positive correlations were observed between biomass estimates derived from the Andrassy formula and the APR (frustum-based) method across all three datasets (Figs. 4–6). Thus, in the Androth/Elikalpeni dataset (Fig. 4), biomass estimates from the two methods showed a strong linear relationship (Pearson's $r = 0.932$, $p < 0.0001$). The mean difference between methods was −0.493 µg (SD = 2.138 µg), indicating that the frustum-based method tended to yield slightly lower biomass values for small to medium-sized nematodes. This subtle but consistent underestimation by the frustum method is likely due to its ability to correct for the slight tapering present even in predominantly cylindrical forms, which the Andrassy model approximates as a uniform cylinder. The narrow spread of differences (SD = 2.138 µg) reflects relatively good agreement across the majority of specimens in this coastal dataset, where nematodes were generally smaller and less morphologically variable. For the Clarion-Clipperton Zone (CCZ) dataset (Fig. 5), the correlation remained high ($r = 0.925$, $p < 0.0001$), with a mean difference of −0.409 µg (SD = 1.879 µg). This close agreement suggests that, for much of the deep-sea nematode community characterized by slender and moderately tapered forms, both methods produce comparable biomass estimates. However, visual inspection of Fig. 5 reveals increasing divergence for larger specimens, where the frustum method begins to generate higher biomass values than Andrassy. This pattern indicates that the Andrassy formula increasingly underestimates biomass in nematodes with greater body size and tapering, a trend more pronounced in the CCZ than in coastal samples due to the presence of larger, robust taxa. The most striking disparity was found in the open source (Nemys) dataset (Fig. 6), which included extremely large and morphologically diverse nematodes. Here, the correlation was strongest ($r = 0.956$ $p < 0.0001$), yet the mean difference reached −251.37 µg (SD = 1096.67 µg). The substantial negative mean difference where the frustum method produced significantly higher biomass estimates than Andrassy highlights a systematic underestimation by the Andrassy formula in large, tapered, or robust nematodes. The wide standard deviation of the differences reflects the high morphological variability in this dataset, with some specimens showing discrepancies exceeding 1000 µg. This result underscores that while both methods are strongly correlated, the Andrassy model fails to accurately scale with increasing body size and morphological complexity, particularly in genera with pronounced anterior or posterior tapering, flared tails, or irregular cross sections.

To further quantify the agreement between the Andrassy and frustum-based (APR formula) biomass estimation methods, Bland-Altman analysis was performed for each dataset (Figs. 7–9). This analysis evaluates both the average difference (bias) and the range of agreement between the two methods, providing insight into their consistency across different nematode sizes and morphologies. In the Androth/Elikalpeni dataset (Fig. 7), the mean difference between methods was small (−0.49 µg), with narrow 95% limits of agreement (LoA: −4.68 to 3.70 µg), indicating strong overall agreement and no substantial fixed bias. This reflects the predominance of small, slender, and cylindrical nematodes in this coastal habitat, for which both methods yield similar biomass estimates. However, even within this narrow range, slight proportional bias was visible, with larger specimens (e.g., *Linhomoeus*) beginning to deviate from the mean difference line. For the Clarion-Clipperton Zone (CCZ) dataset (Fig. 8), the mean difference remained close to zero (−0.41 µg) with moderate LoA (−4.09 to 3.27 µg), suggesting good method agreement for the majority of specimens. Yet, clear outliers were present, particularly in robust, tapered genera such as *Terschellingia longicaudata*, *Halichoanolaimus robustus*, and *Sphaerolaimus*, which fell outside the upper agreement limit. This pattern indicates that as nematode size and tapering increase, the Andrassy formula increasingly underestimates biomass relative to the

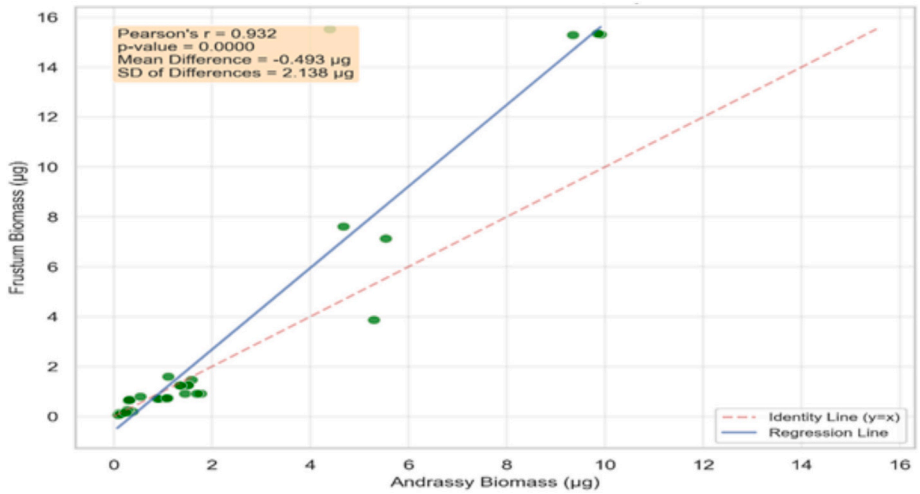

Fig. 4. Correlation between Andrassy and frustum-derived biomass estimates for nematodes from the Androth–Elikalpeni habitat ($n = 50$).

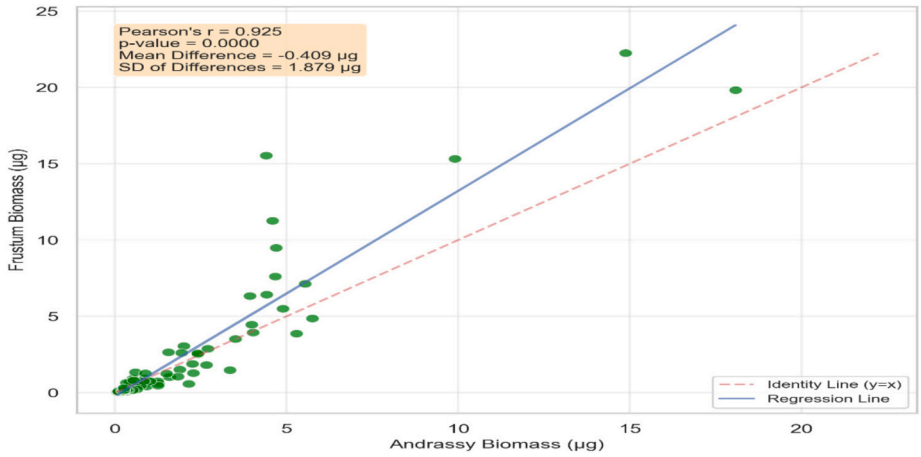

Fig. 5. Correlation between Andrassy and frustum-derived biomass estimates for nematodes from the CCZ habitat (n = 87).

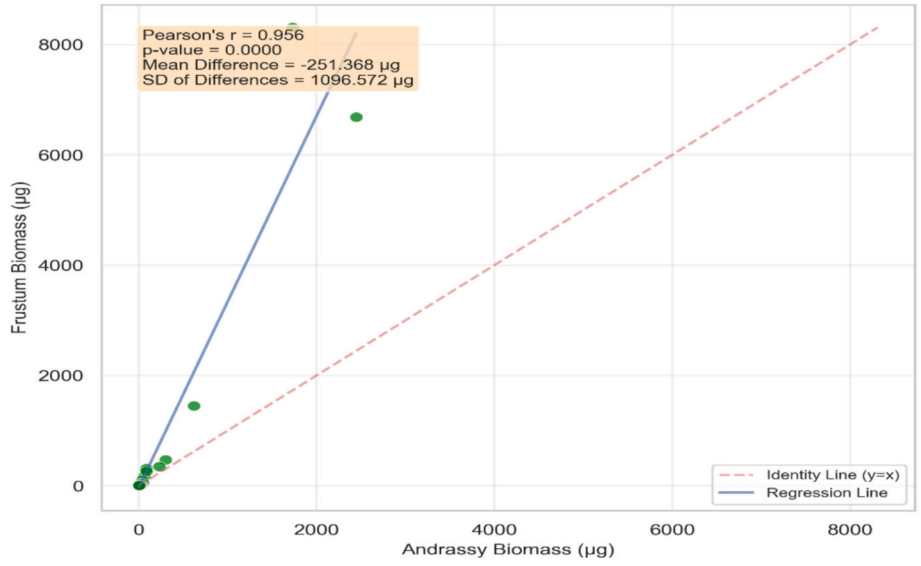

Fig. 6. Correlation between Andrassy and frustum-derived biomass estimates for nematodes from the Open source (Nemys database) (n = 50).

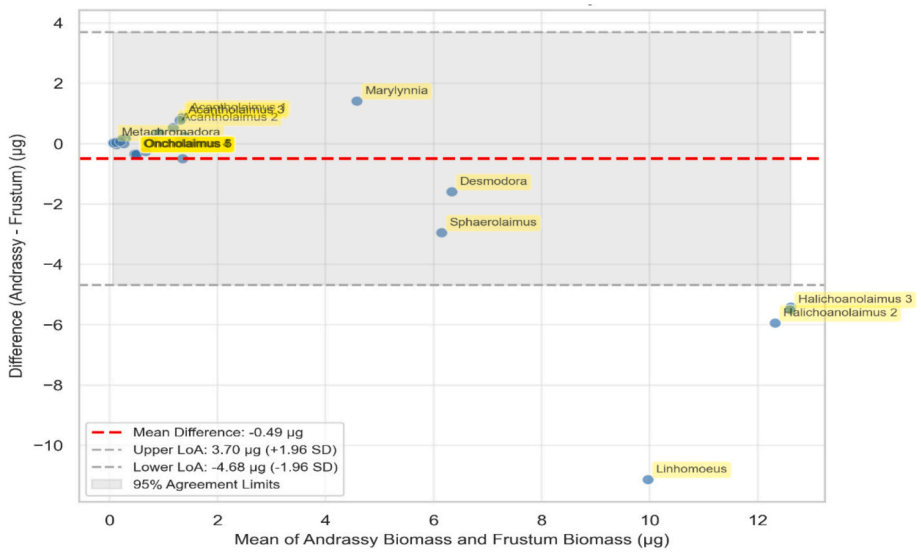

Fig. 7. Bland-Altman plot showing agreement between biomass estimates from the Andrassy and Frustum (The APR Formula) methods for nematodes from Androth/Elikalpeni (n = 50).

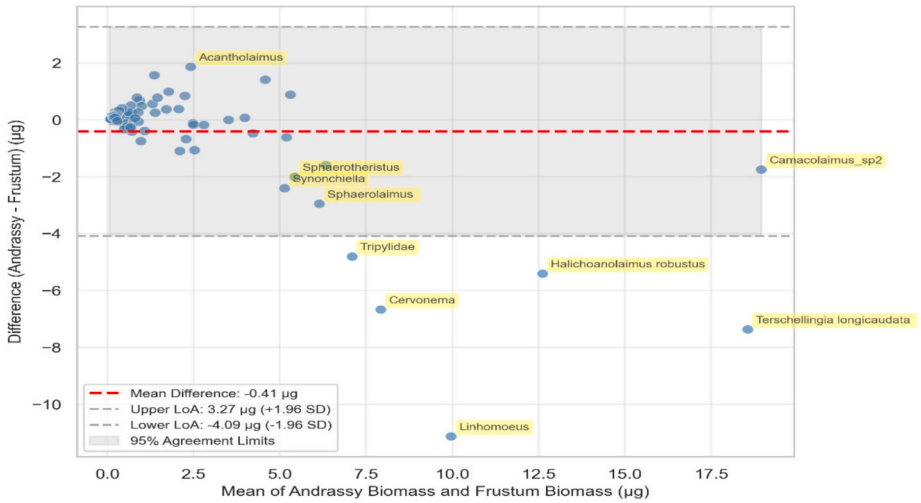

Fig. 8. Bland-Altman plot showing agreement between biomass estimates from the Andrassy and Frustum (The APR Formula) methods for nematodes from CCZ ($n = 87$).

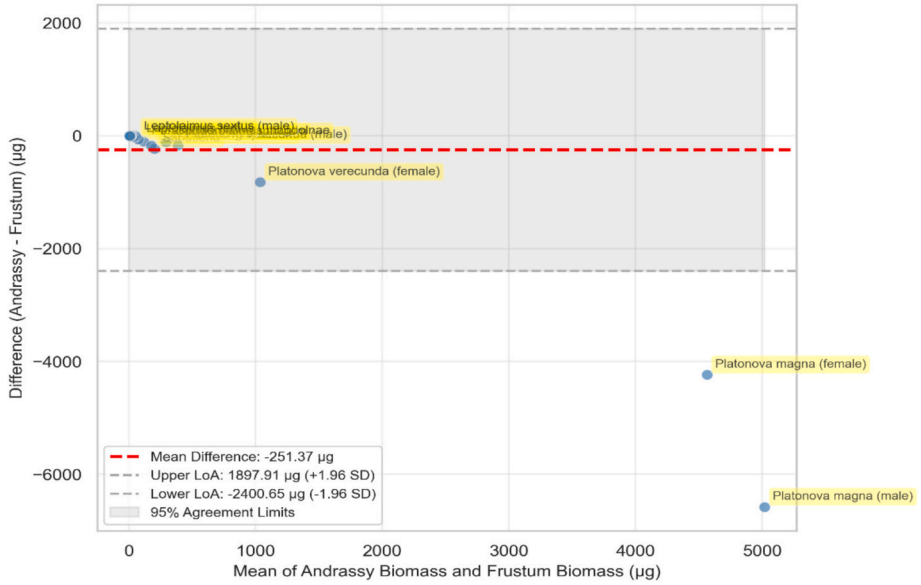

Fig. 9. Bland-Altman plot showing agreement between biomass estimates from the Andrassy and Frustum (The APR Formula) methods for nematodes from Open source ($n = 50$).

frustum-based method. The most pronounced disagreement was observed in the open source (Nemys) dataset (Fig. 9). Here, the mean difference was large and negative (−251.37 µg), with extremely wide LoA (−2400.65 to 1897.91 µg). This substantial bias was driven by several extremely large, morphologically complex taxa, including *Platonova magna* (both male and female) and *Parasphaerolaimus*, which exhibited differences exceeding 1000 µg. These outliers confirm a strong size- and morphology-dependent bias: the Andrassy formula systematically underestimates biomass in large, tapered nematodes, while the frustum method captures their true volumetric scaling more accurately.

3.3. Biomass estimation across morphological groups

A comprehensive and comparative analysis of biomass estimation using the APR and Andrassy methods was conducted across three independent nematode datasets: Androth Elikalpeni, CCZ, and open source. The Supplementary Table S1 provides comprehensive information that includes the detailed genus level comparison of all key morphometric parameters and biomass estimates of each genus from all three datasets. The dataset contains three sheets of nematode morphometric and biomass data. The Androth Elikalpeni sheet includes 50 entries with length, diameter, L/D ratio, morphology type, and biomass calculated by two methods. The CCZ sheet contains 87 entries from the deep-sea Clarion Clipperton Zone, featuring similar measurements but with greater genus and species diversity. The open source sheet compiles 50 published records, including very large specimens and sex-disaggregated data, with biomass values significantly higher than those of the other two sheets. All sheets provide consistent metrics: length, maximum diameter, L/D ratio, morphology classification, segment count, lateral surface area, and biomass estimates using both the Andrassy and Frustum formulas. These datasets collectively reveal significant variability in nematode body size and biomass across marine environments, from coastal regions to the deep sea. While specimens from the Androth Elikalpeni and CCZ datasets generally fall within a moderate size range, the open source data include extreme deep-sea specimens, such as *Platonova magna*, reaching lengths over 2 cm and

biomass estimates exceeding 2400 μg. Biomass calculations differ notably between the Andrassy and Frustum methods, particularly for larger individuals, and morphology classified as stout, medium, or slender based on L/D ratio shows clear environmental and taxonomic trends. Together, these results underscore how habitat influences nematode morphology and biomass, providing a foundation for ecological comparisons and deep-sea biodiversity assessments.

The analysis reveals systematic, morphology- and size-dependent discrepancies between the two methods, with specific genera exhibiting extreme differences that highlight the geometric and biological factors influencing biomass calculation. This analysis also reveals pronounced and statistically significant discrepancies between the Frustum and Andrassy calculation methods. Statistical analysis across all datasets indicates that the Frustum method systematically produces higher biomass estimates (paired *t*-test: $t(186) = 12.47$, $p < 0.001$), with an overall mean Frustum/Andrassy ratio of 1.84 (SD = 1.12) and a mean absolute difference of +37.42 μg (SD = 318.15 μg). These differences exhibit strong morphology-dependent patterns: stout-bodied nematodes show a mean ratio of 1.68 (SD = 0.92, $n = 58$), medium-bodied forms average 1.42 (SD = 0.61, $n = 67$), while slender forms demonstrate the highest mean ratio of 2.42 (SD = 1.89, $n = 62$), though this is inflated by exceptionally long specimens. While several genera including *Wieseria*, *Daptonema*, *Leptolaimus*, *Oncholaimus*, and *Microlaimus* showed minimal differences between methods regardless of habitat, indicating stable geometric proportionality, dramatic positive deviations (Frustum > Andrassy) were concentrated in specific taxa. These included *Linhomoeus* (Androth/Elikalpeni), *Terschellingia* (CCZ), *Halichoanolaimus* (both Androth/Elikalpeni and CCZ), *Parasphaerolaimus* (open source), and extreme large bodied genera such as *Platonova* and *Onchium longispiculum* (open source), where frustum-derived biomass exceeded Andrassy estimates by several fold. Notably, genera within the same morphological class (based on L/D ratio) did not behave uniformly; for instance, slender taxa like *Wieseria* and *Daptonema* exhibited low methodological divergence, whereas other slender taxa like *Linhomoeus* and *Terschellingia* showed large differences. Similarly, among large bodied genera, some (e.g., *Oncholaimus*) displayed low divergence, while others of comparable size showed high divergence. These genus level patterns directly shaped habitat level outcomes.

In the Androth Elikalpeni dataset, dominated by small to medium sized nematodes, the Andrassy method generally produced higher biomass estimates for slender and medium morphotypes (e.g., *Euchromadora*, *Halalaimus*). However, a crucial reversal was observed for stout bodied genera with low length-to-diameter (L/D) ratios. For *Desmodora* (L/D 14.16), the Arjun-Preet-Ravail biomass (7.13 μg) was 29% higher than the Andrassy estimate (5.54 μg), a pattern repeated in *Sphaerolaimus* (L/D 12.31) where APR (7.62 μg) exceeded Andrassy (4.67 μg) by 63%. This indicates that for stout morphologies, the cylindrical simplification of the Andrassy formula leads to significant underestimation compared to the more geometrically accurate frustum model. The CCZ dataset, featuring greater morphological diversity, starkly highlights this dichotomy. For extremely stout forms like *Greeffiella* (L/D 5.18), the frustum biomass (4.67 μg) was 3.7 times greater than the Andrassy estimate (1.25 μg). Similarly, stout *Desmocolex* species showed frustum estimates 1.5–2 times higher. Conversely, for long, slender nematodes like *Terschellingia longicaudata* (L/D 42.88), the Andrassy method yielded a lower estimate (14.88 μg) than frustum (22.25 μg). The extreme outlier *Linhomoeus* (L/D 715.85) further demonstrated the APR method's sensitivity to extreme proportions, calculating a biomass (15.53 μg) 3.5 times larger than Andrassy (4.4 μg). This dataset proves that in a mixed community, reliance on a single method introduces systematic bias for or against specific morphological groups. The open source dataset, containing giant deep-sea nematodes, delivered the most dramatic contrasts. Here, the APR method generated massively higher biomass estimates across nearly all specimens, regardless of L/D ratio. For example, in *Sabatieria* (L/D 34.23), the APR biomass (315.35 μg) was 3.7 times the Andrassy value (85.83 μg). This trend peaked in the largest specimens, such as *Platonova magna* (female), where the frustum estimate (6683.66 μg) was 2.7 times greater than the Andrassy (2445.87 μg). This consistent pattern demonstrates that for macro-sized nematodes, the Andrassy formula catastrophically fails to capture true biovolume, likely due to its inability to account for the significant tapering and complex shape of large organisms (Fig. 10).

3.4. Segmentation analysis (5, 10, 20 Segments)

RAH NemaCalc computed frustum-based biomass for 187 nematode specimens (50 from 34 Androth/Elikalpeni genera, 87 from 41 CCZ genera, and 50 from open source) using 5-, 10-, and 20-segment models to evaluate how tapering and body form influence estimation accuracy. Specimens were categorized by L/D ratio: 5 segments for slender, near-cylindrical forms (>30), 10 for moderately tapered forms (15–30), and 20 for strongly tapered, robust, or segmented forms (<15). High resolution images (1920 × 1080 px, 2 MB) were processed in 1.8 s (10 segments) and 2.1 s (20 segments).

The segmentation analysis revealed that formula performance diverges only when body morphology is explicitly considered. The 5-segment model (mean biomass: 2.18 ± 3.95 μg, CV: 181.2%) underestimated robust, highly tapered genera such as *Terschellingia* (−2.1%) and *Linhomoeus* (−2.6%) due to oversimplified tapering. The 10-segment model (mean: 2.24 ± 4.02 μg, CV: 179.5%) achieved the best trade-off between accuracy and computational time, with <1% deviation for moderately tapered genera (*Marylynnia*, *Viscosia*) and exact estimates for cylindrical forms (*Desmocolex*). The 20-segment model (mean: 2.29 ± 4.08 μg, CV: 178.1%) most accurately captured tapering in large, complex morphologies (e.g., *Halichoanolaimus* at +1.5%, *Terschellingia* at +1.9%), with significant improvement over 10 segments. Slender genera showed negligible changes (<5% variation), confirming that additional segmentation only benefits morphologically complex specimens.

4. Discussion

This study introduces RAH NemaCalc, a novel software tool developed to address critical methodological gaps in marine nematode biomass estimation. The tool was validated using specimens from ecologically distinct habitats, including coastal systems of the Androth/Elikalpeni Islands (Indian Ocean), abyssal sediments of the Clarion-Clipperton Zone (Pacific Ocean), and an open-source global database (Nemys), ensuring its applicability across diverse marine environments and nematode morphotypes. By integrating geometric accuracy with computational efficiency, RAH NemaCalc provides a robust, scalable solution for reliable biomass quantification, supporting more accurate assessments of nematode-mediated ecological functions and anthropogenic impacts. Existing approaches are limited by geometric oversimplifications or lack of adaptability to marine nematode morphologies. The foundational Andrássy formula (1956) applies a universal cylindrical model that fails to account for body tapering, leading to systematic biases. While semi-automated image analysis tools such as those by Baguley et al. (2004) and Mazurkiewicz et al. (2016) improved measurement efficiency, they retained cylindrical or cuboid approximations and offered only taxon-specific corrections. Specialized platforms like NINJA (Sieriebriennikov et al., 2014) rely on preexisting taxon-specific mass data, limiting their accuracy in marine environments where morphological data are scarce. Other methods, such as biomass-size spectra (Vanaverbeke et al., 2003; Vanreusel et al., 1995) and diameter-only simplifications (Zhao et al., 2019), either depend on Andrássy-based inputs or sacrifice morphological accuracy for speed. Recent terrestrial-focused efforts, including the HoliSoils Project (2024) and studies by Li et al. (2023) and Ma et al. (2024a), continue to rely on classical formulas and lack marine applicability. In contrast, RAH NemaCalc implements an automated, morphology-sensitive frustum-based segmentation approach, enabling precise biomass estimation

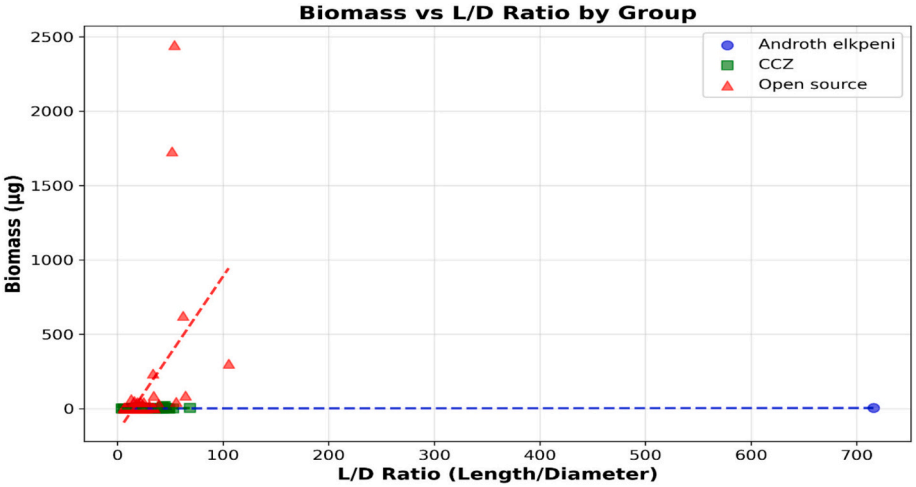

Fig. 10. The analysis shows the significant difference in the dataset of open source due to more morphologically varying nematodes.

Table 4
Comparison of RAH NemaCalc with prior nematode biomass estimation methods.

Study/Software	Habitat	Description	Biomass/Volume Calculation Method	New Formula?
Andrassy (1956)	Terrestrial & Freshwater	Foundational work deriving standard nematode biomass formula using summed cones and truncated cones, simplified for routine use.	Volume: $V = (L \times D^2) / 1.7$ (μm^3) Biomass: $W = (L \times D^2) / (1.6 \times 10^6)$ (µg, fresh weight) L = length (µm), D = max. Diameter (µm) Specific gravity: 1.084	Yes (universal)
Baguley et al. (2004)	Marine	Semi-automated image analysis for nematode morphometry and biomass estimation.	Measures length and width via image analysis; applies Andrassy's formula.	No
ASLO Mazurkiewicz et al. (2016)	Marine	Evaluates biomass formulas, proposing taxon-specific corrections; tests cuboid, cylinder, and Andrassy's formulas via semi-automated image analysis.	Compares Andrassy's, Wieser's, and taxon-specific corrections; tests cuboid: $V = L \times W \times H$ ($H \approx D$); identifies significant biomass differences.	Yes (taxon-specific)
Ghaderi (2020)	Terrestrial (Plant-parasitic)	Database of taxon- and life-stage-specific body-size values for plant-parasitic nematodes.	Uses published length and diameter per taxon/life stage; applies Andrassy's or similar formulas, grouped by morphotype.	No (refinement)
Sieriebriennikov et al. (2014) – NINJA	Terrestrial	Web-based tool for automated nematode biomass and ecological index calculation.	Uses taxon-specific body mass from Nemaplex; multiplies mean body mass by abundance.	No
Vanaverbeke et al. (2003)	Marine	Analyzes nematode biomass spectra (NBS) for benthic communities using size-class distributions.	Measures size; applies Andrassy's formula; constructs $\log_2$-based biomass spectra.	No
Vanreusel et al. (1995)	Marine	Constructs nematode biomass spectra at abyssal sites, linking biomass to food supply and environmental gradients.	Measures length and width; applies Andrassy's formula; uses $\log_2$ size classes.	No
Vranken and Heip (1986)	Marine	Explores nematode productivity; proposes empirical annual P/B ratios.	Uses power law: $P/B = aM^b$ (productivity/biomass ratio, not direct biomass).	Yes (P/B ratio)
Li et al. (2023)	Terrestrial	Examines nematode biomass changes along elevational gradients.	Uses Andrassy's formula and community-weighted mean biomass.	No
Zhao et al. (2019)	Terrestrial	Proposes simplified nematode weight estimation using only diameter (D).	Rapid weight estimation based on diameter, reducing measurement time.	Yes (diameter-based)
Evaluation of Biomass Methods Llopis-Belenguer et al. (2018)	Marine	Compares clay modeling, image analysis, and geometric approximation for small invertebrate biomass, including nematodes.	Tests geometric models (cuboid/cylinder); validates against direct weighing.	Yes (method comparison)
Simplified Soil Nematode Biomass (China Grasslands) Ma et al. (2024b)	Terrestrial	Compare Zhao's simplified formula with Andrassy's for soil nematode biomass.	Simplified formula matches Andrassy; outperforms family-averaged weights.	Yes (simplified)
HoliSoils Project (2024)	Terrestrial	Harmonizes methodologies for nematode biomass quantification in European forest soils; recommends automation.	Uses Andrassy's formula, Nemaplex, and NINJA; recommends morphometric assignment by taxon.	No
Grazing & Resource Availability Andriuzzi and Wall (2018)	Terrestrial	Explores grazing and resource effects on nematode body size, mass, and biomass in semi-arid grasslands.	Measures length, diameter, and mass; uses standard formulas (e.g., Andrassy's).	No
Livestock Grazing Ma et al. (2024a)	Terrestrial	Examines livestock grazing effects on nematode body size and biomass in grassland mosaics.	Measures body size; calculates community-weighted mean biomass using standard methods.	No
Dominant Plants & Grazing Rafael et al. (2023)	Terrestrial	Assesses grazing and plant species effects on nematode morphometric traits in wet meadow grasslands.	Measures length and mass; applies published morphometric/biomass formulas.	No
Present Study	Deep-sea	Semi-automated image analysis tool (RAH NemaCalc) for nematode length, diameter, and biomass using frustum-based segmentation.	Calculates biomass via lateral surface area of frustum segments; sums LSA with correction factors; compares with Andrassy's formula.	Yes (frustum-based)

across a broad spectrum of body shapes (Table 4).

The core finding that biomass estimation error is not random but systematically governed by nematode morphology confirms and quantifies long suspected limitations of the foundational Andrássy formula (Andrassy, 1956). Our results demonstrate a clear morphological continuum of bias: for slender, near-cylindrical taxa, the frustum method corrected the overestimation inherent in the cylindrical model, yielding 28–75% lower biomass. This aligns with observations that simple geometric shapes inflate volume for subtly tapered forms (Vanaverbeke et al., 2003). Conversely, for robust, highly tapered genera, the frustum method produced biomass estimates 128–178% higher than Andrássy, providing the first comprehensive quantitative evidence that the single diameter cylindrical assumption catastrophically fails for morphologically complex marine nematodes, a limitation previously noted but not rigorously measured across diverse taxa (Mazurkiewicz et al., 2016).

The analysis revealed that the influence of morphology on this bias scales with body size. The length-to-diameter (L/D) ratio was a weak predictor of biomass in communities of smaller nematodes but explained significant variation ($R^2 = 0.192$, $p = 0.0015$) in the open-source dataset dominated by large, complex taxa. This indicates that the ecological cost of using simplistic models is highest precisely in deep-sea ecosystems like the Clarion Clipperton Zone, where large bodied nematodes contribute disproportionately to community biomass and where accurate carbon accounting is a most critical concern raised in prior deep-sea studies (Vanreusel et al., 1995; Zeppilli et al., 2015). Bland-Altman analysis robustly validated this proportional bias, showing limits of agreement widening dramatically for larger specimens. This pattern confirms that disagreement stems from geometric limitations rather than random error, a conclusion consistent with validation studies on other morphologically complex meiofauna (Llopis-Belenguer et al., 2018). Importantly, agreement between methods varied among genera within the same morphology class. Genera with marked longitudinal diameter variation (e.g., *Linhomoeus*, *Platonova*) showed large divergence, while those with uniform body profiles (e.g., *Oncholaimus*) showed close agreement. This indicates that L/D ratio alone is an insufficient descriptor and that direct measurement of diameter variability, as done in the frustum approach, is necessary for accuracy. Similar observations that fine scale body shape influences biomass estimates have been reported previously (Soetaert et al., 2009).

RAH NemaCalc advances the field by integrating key innovations that directly remedy these shortcomings. First, its dynamic segmentation into conical frustums (5–20 segments) based on L/D ratio directly captures continuous body taper, overcoming the rigidity of fixed shape models. The segmentation analysis confirmed that while 10 segments offer an optimal balance of speed and accuracy for most forms, 20 segments are necessary for highly tapered genera, demonstrating that accuracy is maximized when segment number aligns with morphology. This adaptable approach captures subtle morphological gradients, including anterior/posterior tapering and cuticular thickening, which are particularly visible in high-resolution imaging. Second, by calculating biomass from the sum of segmental lateral surface areas (LSA) rather than volume alone, the APR formula connects morphology to a physiologically relevant metric tied to metabolic exchange and nutrient uptake (DeLong et al., 2010; Ferris, 2010; Glazier, 2008), moving beyond purely volumetric proxies and addressing a conceptual limitation of volume-only methods (Martins et al., 2014). We further reinforced the robustness of this approach by establishing a narrow, consistent mean density ($\rho = 1.08 \pm 0.05$ g/cm^3) via sucrose gradient centrifugation, confirming that geometric assumptions, not density uncertainty, are the primary source of historical estimation error. Third, the tool achieves a practical breakthrough in efficiency (~2 s per specimen), representing a > 100-fold reduction compared to manual methods (Baguley et al., 2004), thus enabling the high-throughput analysis required for large-scale ecological monitoring.

The correction of systematic biomass underestimation for large, tapered nematodes has profound implications for deep-sea ecology and conservation. In regions like the CCZ, our results suggest that 50% or more may be underreported in historical carbon stock estimates derived from Andrássy-based methods. This substantial revision can alter the perceived role of nematodes in benthic carbon cycling and sequestration, with direct importance for modeling ecosystem function and for establishing environmental baselines in areas targeted for resource extraction, like deep-sea mining (Danovaro et al., 2020; Jones et al., 2017). Furthermore, by providing precise, scalable biomass data, RAH NemaCalc enhances the capacity to detect anthropogenic impacts and track ecosystem health, supporting evidence-based ocean management and conservation (Rabone and Glover, 2023). While representing a significant advance, future integration of fully automated contour detection and exploration of links between LSA-based biomass and metabolic or trophic traits could further elevate the tool's utility and biological insight. While RAH NemaCalc represents a major advance, some limitations remain. Contour tracing, though semi-automated, still requires user input; future integration of AI-driven contour detection could fully automate segmentation. The density value, while consistent across our tested genera, could benefit from broader taxonomic validation. Exploring potential links between LSA, specific metabolic rates, and taxonomic identity could further refine functional biomass proxies. The software's modular architecture readily accommodates such enhancements, including automated segmentation optimization, which could further streamline processing for future high-throughput applications.

5. Conclusion

This study demonstrates that accurate nematode biomass estimation requires both morphological sensitivity and computational efficiency, as achieved by the RAH NemaCalc software. The development and validation of RAH NemaCalc provide a decisive solution to this long-standing methodological challenge. By implementing an automated, frustum-based segmentation approach, the tool directly addresses the core limitation of the classic Andrássy formula, its reliance on a uniform cylindrical shape, which we have shown to introduce predictable and significant errors: overestimating biomass in slender, thread-like nematodes and, more critically, underestimating it by up to 260% in robust, highly tapered taxa commonly found in deep-sea environments. The key insight from our multi-habitat validation is that biomass estimation bias is not random but is a scalable function of nematode body size and shape complexity. The frustum-based Arjun-Preet-Ravail (APR) formula corrects this by dynamically adapting to morphology through segmental lateral surface area calculation, resulting in more biologically realistic estimates. RAH NemaCalc provides the necessary precision, speed, and scalability to meet this need, transforming nematode biomass from a rough proxy into a robust metric. This advancement is critical for generating reliable baselines, monitoring anthropogenic impacts such as deep-sea mining, and ultimately supporting evidence-based conservation of vulnerable marine ecosystems. By bridging the gap between geometric simplification and biological reality, this work establishes a new standard for quantifying the functional role of the ocean's most abundant metazoans.

CRediT authorship contribution statement

Harshpreet Kaur: Writing – original draft, Formal analysis, Data curation. **Arjunveer Singh:** Validation, Software, Methodology, Investigation, Formal analysis, Data curation. **Daniel Jones:** Validation, Methodology. **Pedro Martinez Arbizu:** Validation. **Ravail Singh:** Writing – review & editing, Visualization, Supervision, Conceptualization.

Declaration of competing interest

The authors declare that they have no conflict of interest.

Acknowledgments

This work was the part of UK Natural Environment Research council (NERC) Seabed Mining And Resilience to Experimental Impact (SMARTEX) project (Grant Reference NE/T003537/1). The corresponding author carried out this research at the National Oceanography Centre (NOC), UK. We extend our sincere thanks to the Director of NOC and the Head of Department for their support and facilitation during this work. We also acknowledge the Deep Ocean Mission project for building the nematode dataset used in this study.

Appendix A. Supplementary data

Supplementary data to this article can be found online at https://doi.org/10.1016/j.ecoinf.2026.103728.

Data availability

All image datasets and illustrations are provided in Supplementary File 1. The complete software architecture, framework, and step-by-step operational workflow of RAH NemaCalc are described in detail in Supplementary File 2. The step by step guide for using RAH NemaCalc is available in Supplementary File 3. This document provides comprehensive information. A detailed genus-level comparison of all key morphometric parameters and biomass estimates of each genera from all the three datasets is provided in Supplementary Table S1.The software along with all the codes/data is open-source and freely available at https://github.com/ArjunXY/RAH_NemaCalc.

References

Andrassy, I., 1956. Die rauminhalts-und gewichtsbestimmung der fadenwürmer (Nematoden). Acta Zoologica Hungarica 2 (1), 1–5.

Andriuzzi, W.S., Wall, D.H., 2018. Grazing and resource availability control soil nematode body size and abundance–mass relationship in semi-arid grassland. J. Anim. Ecol. 87 (5), 1407–1417. https://doi.org/10.1111/1365-2656.12858.

Baguley, J.G., Hyde, L.J., Thistle, D., 2004. A semi-automated digital microphotographic approach to measure meiofaunal biomass. Mar. Ecol. Prog. Ser. 274, 97–106. https://doi.org/10.4319/lom.2004.2.181.

Danovaro, R., Fanelli, E., Aguzzi, J., Billett, D., Carugati, L., Corinaldesi, C., Yasuhara, M., 2020. Ecological variables for developing a global deep-ocean monitoring and conservation strategy. Nat. Ecol. Evol. 4 (2), 181–192. https://doi.org/10.1038/s41559-019-1091-z.

DeLong, J.P., Okie, J.G., Moses, M.E., Sibly, R.M., Brown, J.H., 2010. Shifts in metabolic scaling, production, and efficiency across major evolutionary transitions of life. Proc. Natl. Acad. Sci. 107 (29), 12941–12945. https://doi.org/10.1073/pnas.1007783107.

Feller, R.J., Warwick, R.M., 1988. Energetics. In: Higgins, R.P., Thiel, H. (Eds.), Introduction to the Study of Meiofauna. Smithsonian Institution Press, pp. 181–196.

Ferris, H., 2010. Form and function: metabolic footprints of nematodes in the soil food web. Eur. J. Soil Biol. 46 (2), 97–104. https://doi.org/10.1016/j.ejsobi.2010.01.003.

Fonseca, G., Soltwedel, T., 2007. Deep-sea meiobenthic communities underneath the marginal ice zone off eastern Greenland. Polar Biol. 30 (5), 607–618. https://doi.org/10.1007/s00300-006-0220-8.

Ghaderi, R., 2020. Biomass calculation for plant-parasitic nematodes reveals variability across genera of the same family. Nematology 23 (4), 367–379. https://doi.org/10.1163/15685411-bja10047.

Giere, O., 2009. Meiobenthology: The Microscopic Motile Fauna of Aquatic Sediments, 2nd ed. Springer. https://doi.org/10.1007/978-3-540-68661-3.

Glazier, D.S., 2008. Effects of metabolic level on the body size scaling of metabolic rate in birds and mammals. Proc. R. Soc. B Biol. Sci. 275 (1641), 1405–1410. https://doi.org/10.1098/rspb.2008.0118.

Heip, C., Vincx, M., Vranken, G., 1985. The ecology of marine nematodes. Oceanogr. Mar. Biol. Annu. Rev. 23, 399–489.

HoliSoils Project, 2024. Harmonised Methodologies for Quantification of Biomass of Key Trophic Groups. https://holisoils.eu/wp-content/uploads/2024/05/D1.3-Harmonised-methodologies-for-quantification-of-biomass-of-key-trophic-groups.pdf.

Jones, D.O.B., Kaiser, S., Sweetman, A.K., Smith, C.R., Menot, L., Vink, A., Trueblood, D., Greinert, J., Billett, D.S.M., Arbizu, P.M., Radziejewska, T., Singh, R., Ingole, B., Stratmann, T., Simon-Lledó, E., Durden, J.M., Clark, M.R., 2017. Biological responses to disturbance from simulated deep-sea polymetallic nodule mining. PLoS One 12 (2), e0171750. https://doi.org/10.1371/journal.pone.0171750.

Li, G., Wilschut, R.A., Luo, S., Chen, H., Wang, X., Du, G., Geisen, S., 2023. Nematode biomass changes along an elevational gradient are trophic group dependent but independent of body size. Glob. Chang. Biol. 29 (17), 4898–4909. https://doi.org/10.1111/gcb.16814.

Llopis-Belenguer, C., Blasco-Costa, I., Balbuena, J.A., 2018. Evaluation of three methods for biomass estimation in small invertebrates, using three large disparate parasite species as model organisms. Sci. Rep. 8 (1), 3897. https://doi.org/10.1038/s41598-018-22304-x.

Ma, Q., Zhu, Y., Chen, Y., Wu, W., Qing, X., Liu, T., Liu, J., Wang, L., Wu, D., Wang, L., 2024a. Simplified estimates of soil nematode body mass using maximum diameter: insights from large-scale grasslands across China. Soil Biol. Biochem. 191, 109349. https://doi.org/10.1016/j.soilbio.2024.109349.

Ma, Q., Zhu, Y., Wang, Y., Liu, T., Qing, X., Liu, J., Liu, J., Wang, L., Wu, D., Zhang, L., Chen, Y., Wang, L., 2024b. Livestock grazing modifies soil nematode body size structure in mosaic grassland habitats. J. Environ. Manag. 351, 119600. https://doi.org/10.1016/j.jenvman.2023.119600.

Martins, R.T., Melo, A.S., Gonçalves Jr., J.F., Hamada, N., 2014. Estimation of dry mass of caddisflies *Phylloicus elektoros* (Trichoptera: Calamoceratidae) in a Central Amazon stream. Zoologia 31 (4), 337–342. https://doi.org/10.1590/S1984-46702014000400005.

Mazurkiewicz, M., Górska, B., Jankowska, E., Włodarska-Kowalczuk, M., 2016. Assessment of nematode biomass in marine sediments: a semi-automated image analysis method. Limnol. Oceanogr. Methods 14 (12), 816–827. https://doi.org/10.1002/lom3.10128Digital Object Identifier (DOI).

Miljutin, D.M., Miljutina, M.A., Arbizu, P.M., Galéron, J., 2011. Deep-sea nematode assemblage has not recovered 26 years after experimental mining of polymetallic nodules (clarion-Clipperton fracture zone, tropical eastern Pacific). Deep Sea Res. Part 1 Oceanogr. Res. Pap. 58 (8), 885–897. https://doi.org/10.1016/j.dsr.2011.06.003.

Rabone, M., Glover, A.G., 2023. CCZ Biodiversity Synthesis & DeepData Review Final Report. International Seabed Authority.

Rafael, O., Victory, C., Ryan, N., 2023. Dominant plants mediate effects of grazing on soil nematode traits in a wet meadow grassland. Appl. Soil Ecol. 191, 105047. https://doi.org/10.1016/j.apsoil.2023.105047.

Ridall, A., Ingels, J., 2021. Suitability of free-living marine nematodes as bioindicators: status and future considerations. Front. Mar. Sci. 8, 685327. https://doi.org/10.3389/fmars.2021.685327.

Schindelin, J., Arganda-Carreras, I., Frise, E., Kaynig, V., Longair, M., Pietzsch, T., Preibisch, S., Rueden, C., Saalfeld, S., Schmid, B., Tinevez, J.-Y., White, D.J., Hartenstein, V., Eliceiri, K., Tomancak, P., Cardona, A., 2012. Fiji: an open-source platform for biological-image analysis. Nat. Methods 9 (7), 676–682. https://doi.org/10.1038/nmeth.2019.

Schratzberger, M., Ingels, J., 2018. Meiofauna matters: the roles of meiofauna in benthic ecosystems. J. Exp. Mar. Biol. Ecol. 502, 12–25. https://doi.org/10.1016/j.jembe.2017.01.007.

Sieriebriennikov, B., Ferris, H., de Goede, R.G.M., 2014. NINJA: an automated calculation system for nematode-based biological monitoring. Ecol. Indic. 36, 494–498. https://doi.org/10.1016/j.ejsobi.2014.02.004.

Singh, R., Miljutin, D.M., Miljutina, M.A., Martinez Arbizu, P., Ingole, B.S., 2014. Deep-sea nematode assemblages from a commercially important polymetallic nodule area in the Central Indian Ocean Basin. Mar. Biol. Res. 10 (9), 906–916. https://doi.org/10.1080/17451000.2013.866251.

Singh, R., Miljutin, D.M., Vanreusel, A., Radziejewska, T., Miljutina, M.M., Tchesunov, A., et al., 2016. Nematode communities inhabiting the soft deep-sea sediment in polymetallic nodule fields: do they differ from those in the nodule-free abyssal areas? Mar. Biol. Res. 12 (4), 345–359. https://doi.org/10.1080/17451000.2016.1148822.

Singh, R., Sautya, S., Ingole, B.S., 2019. The community structure of the deep-sea nematode community associated with polymetallic nodules in the Central Indian Ocean Basin. Deep-Sea Res. II Top. Stud. Oceanogr. 161, 16–28. https://doi.org/10.1016/j.dsr2.2018.07.009.

Snelgrove, P.V.R., Soetaert, K., Solan, M., Thrush, S., Wei, C.-L., Danovaro, R., et al., 2018. Global carbon cycling on a heterogeneous seafloor. Trends Ecol. Evol. 33 (2), 96–105. https://doi.org/10.1016/j.tree.2017.11.004.

Soetaert, K., Muthumbi, A., Heip, C., 2009. Size and shape of ocean margin nematodes: morphological diversity and depth-related patterns. Mar. Ecol. Prog. Ser. 379, 99–109. https://doi.org/10.3354/meps242179.

Vanaverbeke, J., Steyaert, M., Soetaert, K., Rousseau, V., Van Gansbeke, D., Parent, J.Y., Vincx, M., 2003. Nematode biomass spectra as descriptors of functional changes due to human and natural impact. Mar. Ecol. Prog. Ser. 249, 157–170. https://doi.org/10.3354/meps249157.

Vanreusel, A., Vincx, M., Bett, B.J., Rice, A.L., 1995. Nematode biomass spectra at two abyssal sites in the NE Atlantic with a contrasting food supply. Internationale Revue der gesamten Hydrobiologie und Hydrographie 80 (2), 287–296. https://doi.org/10.1002/iroh.19950800215.

Vranken, G., Heip, C., 1986. The productivity of marine nematodes. Ophelia 26 (3), 429–442. https://doi.org/10.1080/00785326.1986.10422004.

Zeppilli, D., Sarrazin, J., Leduc, D., Arbizu, P.M., Fontaneto, D., Fontanier, C., et al., 2015. Is the meiofauna a good indicator for climate change and anthropogenic impacts? Mar. Biodivers. 45 (4), 505–535. https://doi.org/10.1007/s12526-015-0359-z.

Zeppilli, D., Leduc, D., Fontanier, C., Fontaneto, D., Fuchs, S., Gooday, A.J., et al., 2018. Characteristics of meiofauna in extreme marine ecosystems: a review. Mar. Biodivers. 48 (1), 35–71. https://doi.org/10.1007/s12526-017-0815-z.

Zhao, J., Xiao, J., Zhang, W., Fu, Z., Zhang, M., Liu, T., Wang, K., 2019. A method for estimating nematode body lengths for use in the calculation of biomass via a simplified formula. Soil Biol. Biochem. 134, 36–41. https://doi.org/10.1016/j.soilbio.2019.03.021.

Glossary

Andrassy formula: Traditional method for estimating nematode volume and biomass using a simplified cylindrical model, calculated as $V = L \times D^2/1.7$ or biomass as $L \times D^2/1.6 \times 10^{-6}$, where L is length and D is diameter.

Benthic ecosystems: Sediment-based marine habitats at the ocean floor where nematodes dominate meiofauna, driving nutrient cycling and organic matter decomposition.

Biomass: Total mass of living nematodes, typically in micrograms per individual, serving as a proxy for ecological function, carbon standing stock, and environmental impact assessment.

Clarion-Clipperton Zone (CCZ): Abyssal plain in the Pacific Ocean (11–14°N, 116–120°W) at 4100–4400 m depth, rich in polymetallic nodules and targeted for deep-sea mining.

Conical frustum: Truncated cone segment used in RAH NemaCalc to model nematode body sections, enabling precise lateral surface area (LSA) calculation via $AL = \pi(r_1 + r_2)l$, where r_1, r_2 are radii and l is slant height.

Frustum Geometry Factor (f): Correction term in the Arjun-Preet-Ravail (APR) formula, approximating volume from LSA as $f = \frac{1}{3}\frac{r_1^2 + r_1 r_2 + r_2^2}{r_1 + r_2}$ for minimal taper per segment.

Lateral Surface AreaBiomass: External surface area of nematode body segments summed across frustums, basis for biomass. in APR formula: $W = \pi \times k_{total} \times \sum (AL \times f) \times 1.08 \times 10^{-6}$ µg.

Length-Diameter ratio (LD): Morphometric index classifying nematodes as slender (LD $\geq$ 30), moderately tapered (15–30), or robust/highly tapered (LD $<$ 15), driving method-specific biomass bias.

Meiofauna: Small benthic invertebrates (20–500 µm) passing 0.5 mm sieves but retained on 32–63 µm meshes; nematodes comprise up to 90% in marine sediments.

Nematodes: Unsegmented, cylindrical roundworms (phylum Nematoda) abundant in marine benthos, key for nutrient cycling, energy transfer, and as bioindicators of pollution or mining impacts.

RAH NemaCalc: Python-based open-source software using Tkinter GUI and OpenCV for semi-automated nematode morphometrics, frustum segmentation (5–20 segments), and biomass/volume estimation.

Specific gravity: Density relative to water (measured via sucrose gradient centrifugation), empirically 1.05–1.15 g/cm^3 for marine nematodes, averaged at 1.08 g/cm^3 for biomass conversion.